

## Study of penetrating cosmic ray muons and search for large scale anisotropies at the Gran Sasso Laboratory

MACRO Collaboration

S.P. Ahlen <sup>a</sup>, M. Ambrosio <sup>b</sup>, G. Auremma <sup>c,1</sup>, A. Baldini <sup>d</sup>, G.C. Barbarino <sup>b</sup>, B. Barish <sup>e</sup>,  
G. Battistoni <sup>f</sup>, R. Bellotti <sup>g</sup>, C. Bemporad <sup>d</sup>, P. Bernardini <sup>h</sup>, H. Bilokon <sup>f</sup>, V. Bisi <sup>1</sup>, C. Bloise <sup>f</sup>,  
C. Bower <sup>j</sup>, F. Cafagna <sup>g</sup>, M. Calicchio <sup>g</sup>, P. Campana <sup>f</sup>, S. Cecchini <sup>k,2</sup>, V. Chiarella <sup>f</sup>,  
P. Chrysiopoulou <sup>c</sup>, S. Coutu <sup>e</sup>, I.D'Antone <sup>k</sup>, C. De Marzo <sup>g</sup>, G. De Cataldo <sup>g</sup>,  
M. De Vincenzi <sup>c</sup>, O. Erriquez <sup>g</sup>, C. Favuzzi <sup>g</sup>, D. Ficenc <sup>a</sup>, V. Flaminio <sup>d</sup>, C. Forti <sup>f</sup>,  
G. Giacomelli <sup>k</sup>, G. Giannini <sup>d,3</sup>, N. Giglietto <sup>g</sup>, P. Giubellino <sup>1</sup>, M. Grassi <sup>d</sup>, P. Green <sup>l,4</sup>,  
A. Grillo <sup>f</sup>, F. Guarino <sup>b</sup>, E. Hazen <sup>a</sup>, R. Heinz <sup>j</sup>, J. Hong <sup>c</sup>, E. Iarocci <sup>f,5</sup>, S. Klein <sup>a</sup>,  
E. Lamanna <sup>c</sup>, C. Lane <sup>m</sup>, D. Levin <sup>a</sup>, P. Lipari <sup>c</sup>, G. Liu <sup>c</sup>, M. Longo <sup>n</sup>, G. Mancarella <sup>h</sup>,  
G. Mandrioli <sup>k</sup>, A. Marin <sup>a</sup>, A. Marini <sup>f</sup>, G. Martellotti <sup>c</sup>, A. Marzari-Chiesa <sup>1</sup>, M. Maserà <sup>1</sup>,  
P. Matteuzzi <sup>k</sup>, L. Miller <sup>j</sup>, P. Monacelli <sup>o</sup>, M. Monteno <sup>1</sup>, S. Mufson <sup>j</sup>, J. Musser <sup>n</sup>, E. Nappi <sup>g</sup>,  
G. Osteria <sup>b</sup>, B. Pal <sup>k</sup>, O. Palamara <sup>h</sup>, M. Pasquale <sup>1</sup>, V. Patera <sup>f</sup>, L. Patrizii <sup>k</sup>, R. Pazzi <sup>d</sup>,  
C. Peck <sup>c</sup>, J. Petrakis <sup>j</sup>, S. Petrera <sup>c</sup>, L. Petrillo <sup>c</sup>, P. Pistilli <sup>h</sup>, F. Predieri <sup>k</sup>, L. Ramello <sup>1</sup>,  
J. Reynoldson <sup>p</sup>, F. Ronga <sup>f</sup>, G. Rosa <sup>c</sup>, G.L. Sanzani <sup>k</sup>, L. Satta <sup>f,6</sup>, A. Sciubba <sup>c,5</sup>,  
P. Serra-Lugaresi <sup>k</sup>, M. Severi <sup>c</sup>, C. Smith <sup>n</sup>, D. Solie <sup>e</sup>, P. Spinelli <sup>g</sup>, M. Spinetti <sup>f</sup>, M. Spurio <sup>k</sup>,  
J. Steele <sup>e</sup>, R. Steinberg <sup>m</sup>, J.L. Stone <sup>a</sup>, L.R. Sulak <sup>a</sup>, A. Surdo <sup>h</sup>, G. Tarlè <sup>n</sup>, V. Valente <sup>f</sup>,  
R. Webb <sup>q</sup> and W. Worstell <sup>a</sup>

<sup>a</sup> *Physics Department of Boston University, Boston, MA 02215, USA*

<sup>b</sup> *Dipartimento di Fisica dell'Università di Napoli and INFN, I-80125 Naples, Italy*

<sup>c</sup> *Dipartimento di Fisica dell'Università di Roma and INFN, I-00185 Rome, Italy*

<sup>e</sup> *California Institute of Technology, Pasadena, CA 91125, USA*

<sup>d</sup> *Dipartimento di Fisica dell'Università di Pisa and INFN, I-56010 Pisa, Italy*

<sup>f</sup> *Laboratori Nazionali di Frascati dell'INFN, I-00044 Frascati (Rome), Italy*

<sup>g</sup> *Dipartimento di Fisica dell'Università di Bari and INFN, I-70126 Bari, Italy*

<sup>h</sup> *Dipartimento di Fisica dell'Università di Lecce and INFN, I-73100 Lecce, Italy*

<sup>1</sup> *Dipartimento di Fisica dell'Università di Torino and INFN, I-10125 Turin, Italy*

<sup>j</sup> *Department of Physics and Department of Astronomy, Indiana University, Bloomington, IN 47405, USA*

<sup>k</sup> *Dipartimento di Fisica dell'Università di Bologna and INFN, I-40126 Bologna, Italy*

<sup>l</sup> *Department of Physics of Texas A&M University, College Station, TX 77843, USA*

<sup>m</sup> *Department of Physics, Drexel University, Philadelphia, PA 19104, USA*

<sup>n</sup> *Department of Physics of the University of Michigan, Ann Arbor, MI 48109, USA*

<sup>o</sup> *Dipartimento di Fisica dell'Università dell'Aquila and INFN, I-67100 L'Aquila, Italy*

<sup>p</sup> *Laboratori Nazionali del Gran Sasso dell'INFN, I-67010 Assergi (L'Aquila), Italy*

Received 23 April 1990

<sup>1</sup> Also at Università della Basilicata, I-85100 Potenza, Italy

<sup>2</sup> Also at Istituto TESRE/CNR, Bologna, Italy

<sup>3</sup> Also at Università di Trieste, I-34100 Trieste, Italy

<sup>4</sup> Present address: Division 9321, Sandia National Laboratory, Albuquerque, NM 87185, USA.

<sup>5</sup> Also at Dipartimento di Energetica, Università di Roma, I-00185 Rome, Italy

<sup>6</sup> Also at Università dell'Aquila, I-67100 L'Aquila, Italy

The MACRO detector, located in the underground Gran Sasso Laboratory, had its initial data run from February 27 to May 30, 1989, using the first supermodule ( $S\Omega \sim 800 \text{ m}^2 \text{ sr}$ ). Approximately 245 000 muon events were recorded. Here are reported the results of the analysis of penetrating muons which determine the measured vertical muon flux at depths greater than 3000 m.w.e. In addition the data have been used to search for large scale anisotropies

## 1. Introduction

The MACRO (Monopole, Astrophysics, Cosmic Ray Observatory) detector is located in Hall B of the Gran Sasso National Laboratory (LNGS) [1]. This laboratory is at latitude  $42^\circ 27' \text{ N}$ , longitude  $13^\circ 34' \text{ E}$ , average depth of 3800 m of water equivalent (m.w.e.), minimum depth 3000 m.w.e., and at 963 m above sea level. When completed, the MACRO detector will have dimensions  $72 \text{ m} \times 12 \text{ m} \times 10 \text{ m}$ , providing an acceptance for isotropic particle fluxes of  $S\Omega \sim 10\,000 \text{ m}^2 \text{ sr}$  [2–4].

MACRO has been primarily designed to conduct a sensitive search for supermassive grand unified magnetic monopoles. When completed, MACRO will collect  $\sim 10^7$  penetrating muon events per year. Hence, cosmic ray physics with high energy muons can be investigated systematically with high statistics.

This letter presents the analysis of  $\sim 245\,000$  downward going muons obtained during the first run of the first supermodule from February 27 to May 30, 1989, for a total live-time of 1890 h.

## 2. The detector

Two of the primary considerations in the design of the MACRO detector were modularity and redundancy. The final detector will consist of twelve supermodules in two levels, each instrumented to operate independently of the others. This design allows completed sections of the detector to collect data, while other sections are under construction or undergoing tests.

Fig. 1 shows the schematic of one MACRO supermodule. Each supermodule consists of a sandwich array of two layers of liquid scintillation counters (top and bottom) and ten layers of streamer tubes separated by  $32 \text{ cm}$  ( $\sim 60 \text{ g cm}^{-2}$ ) of rock absorbers. In addition, a layer of track-etch plastics (CR39 and lexan) is located across the center plane of the lower supermodule [4]. The sides and two extreme ends of

the detector are covered with one layer of scintillators and six layers of streamer tubes. Fig. 1 shows a general schematic of one MACRO supermodule (lower level), which has dimensions  $12 \text{ m} \times 12 \text{ m} \times 4.8 \text{ m}$  and  $S\Omega \approx 800 \text{ m}^2 \text{ sr}$ .

The streamer tube system consists of  $\approx 5000$  wires per supermodule [2]. Eight tubes, each having dimensions  $3 \text{ cm} \times 3 \text{ cm} \times 12 \text{ m}$ , are combined in a single chamber. The tubes utilize  $100 \mu\text{m}$  anode wires and a graphite cathode. The tubes operate in the limited streamer regime, at present with a gas mixture of Ar (70%),  $\text{CO}_2$  (5%) and *n*-pentane (25%). A two-dimensional readout is performed using signals from the anode wires (X-view) and  $26.5^\circ$  stereo pickup strips (D-view). The overall tube efficiency is 97% (the loss being essentially due to the tube wall thickness). The pickup strips have 98% efficiency relative to the wires. Spatial accuracies for the two views, determined by selecting muon tracks crossing ten horizontal planes, are  $\sigma_x = 1.1 \text{ cm}$  and  $\sigma_D = 1.2 \text{ cm}$ . An angular accuracy for an individual track of  $\approx 0.1^\circ$  can be derived from the spatial accuracy, this is better than the precision with which a reconstructed muon direction can point to the sky, since multiple scattering of muons in the rock overburden dominates. A measure of the overall accuracy obtained from the angular difference between pairs of muons within the same muon bundle gave  $\sigma_\theta \approx 0.6^\circ$ .

The liquid scintillator counters provide accurate measurements of the energy loss and of the velocity of crossing particles [3]. The horizontal layers consist of PVC tanks ( $12 \text{ m} \times 75 \text{ cm} \times 25 \text{ cm}$ ) lined with FEP teflon filled with liquid scintillator and equipped with two 20 cm diameter hemispherical photomultipliers (PMTs) at each end. The vertical layers, which close the sides and ends of the detector, are made of tanks with dimensions of  $12 \text{ m} \times 50 \text{ cm} \times 24 \text{ cm}$  that are viewed by one PMT at each end. The liquid scintillator is based on an ultra-pure low paraffin mineral oil with a mixture of pseudocumene, PPO, wavelength shifters, and anti-oxidant. The optimization of

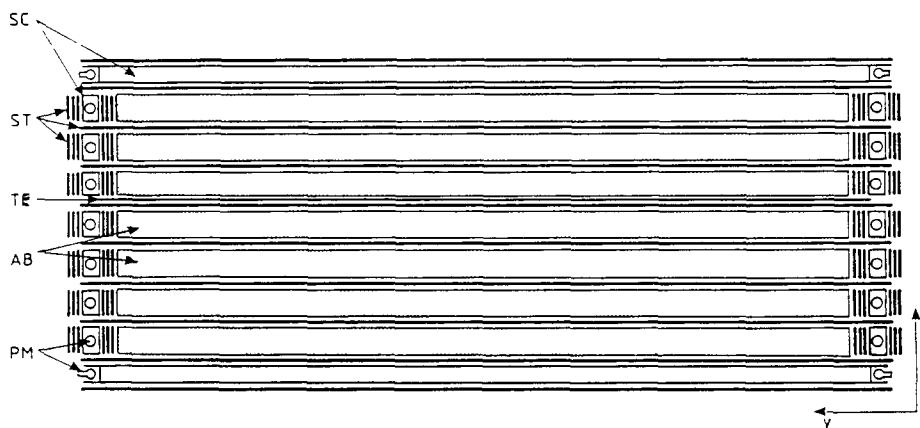


Fig 1 A schematic drawing of the lower level of one MACRO supermodule  $12\text{ m} \times 12\text{ m} \times 4.8\text{ m}$  SC=scintillators, ST=streamer tubes, TE=track-etch, AB=absorbers, PM=photomultipliers

the mixture and a careful selection of all the ingredients has resulted in both a good light yield and a measured attenuation length in the range of 12–14 m. A relativistic muon traversing the counter yields more than a hundred photoelectrons in each end. The scintillator/PMT readout system consists of TDCs and ADCs on the PMT anode and on one dynode, covering a dynamic range of pulse heights up to 10 000 photoelectrons. Analog and digital systems reconstruct the energy deposited in a counter, independently of impact point, down to a threshold of 5 MeV. Slow (20 MHz) and fast (50 MHz) waveform digitizers record the pulse heights versus time and hence the energy loss and velocity of slow and fast particles crossing the counters. The measured time resolution at a single end of the counters, averaged over the initial running period and over all the counters, is  $\sigma_t = 1.7$  ns. This is more than adequate to distinguish upward-going from downward-going muons.

Several muon triggers have been implemented in the first supermodule to detect relativistic penetrating particles in both the streamer tube and scintillator systems. The streamer tube trigger requires a six out of ten horizontal layer majority or a seven out of twenty plane majority when the vertical planes are included. The scintillator trigger requires a coincidence between photomultipliers within a single tank. A mixed trigger was also implemented with lower requirements on both streamer tubes and scintillators. The overall rate on these triggers, largely overlap-

ping, is 0.1 Hz. About one in three triggers is a good muon event; the remaining triggers result primarily from radioactive background. Specialized triggers for the detection of slow particles (monopoles) and of neutrinos from stellar collapses have also been implemented.

The data acquisition system includes a network (Ethernet-DECNET) of Micro VAXs acting as a front-end to the (CAMAC) digitizing electronics and it runs in the VAXELN environment [5]. A central VAX-8200 computer is used as a file server and as an interface between the acquisition system and the users' world.

### 3. Results

#### 3.1 Vertical muon flux

A subsample of throughgoing muons has been selected with the requirement that the muon trajectory cross the apparatus from the top horizontal layer to the bottom horizontal layer of the streamer tubes ( $S\Omega \approx 200\text{ m}^2\text{ sr}$ ). The cuts selected a subsample of 96 000 muons. The zenith and azimuthal distributions of the selected events corrected for acceptance are shown in fig. 2. The maximum of the zenith angle distribution is shifted from the vertical, due to the mountain overburden.

In order to calculate the dependence of the vertical

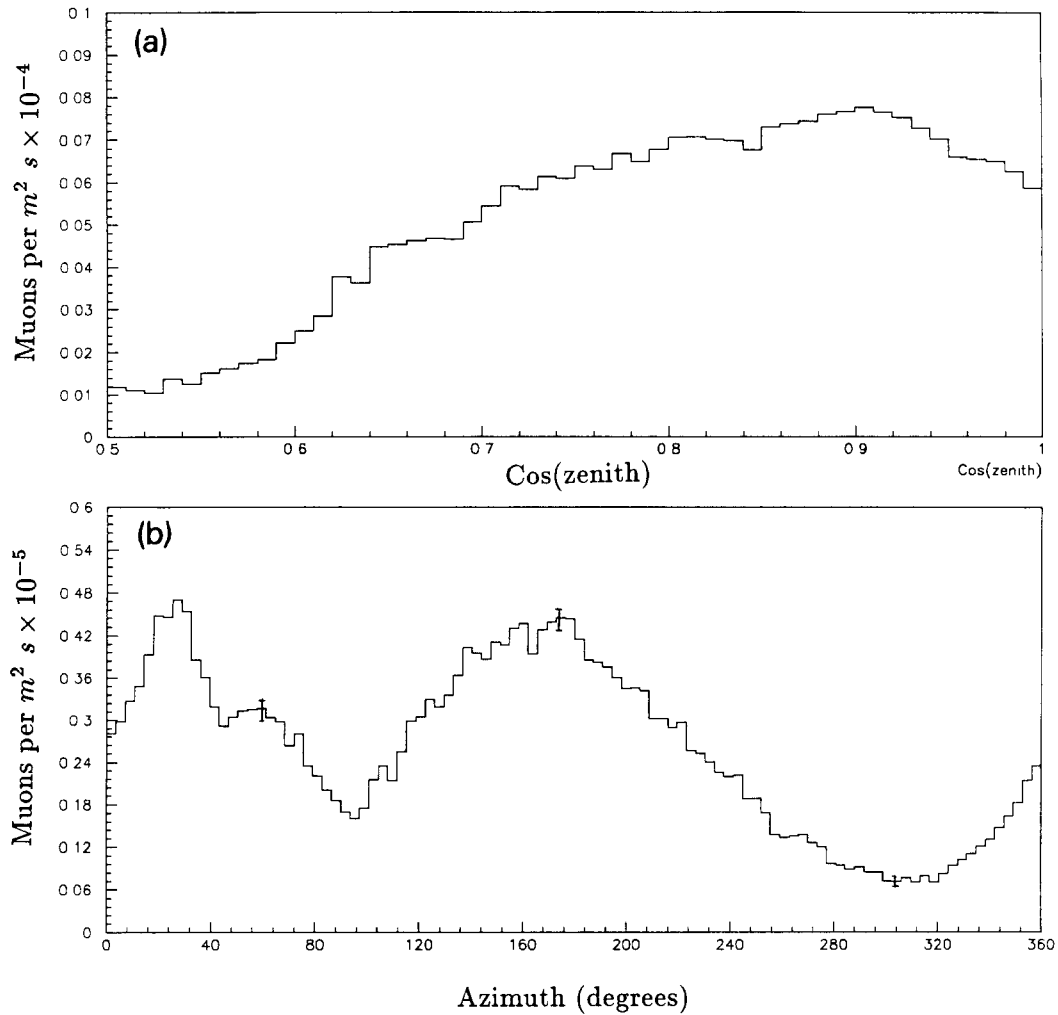


Fig 2 Measured zenith (a) and azimuth (b) distributions of muons crossing ten horizontal planes of the MACRO detector corrected for detector acceptance ( $\Delta\phi=3.6^\circ$ ,  $\Delta\cos\theta=0.01$ ). Some typical statistical errors are shown

muon flux on depth, the sample has been subdivided into bins of equal solid angle  $\Delta\Omega$  ( $\Delta\phi=3.6^\circ$ ,  $\Delta\cos\theta=0.01$ ). Assuming that the zenith angle dependence of the intensity is of the form  $I(h, \theta) = I_0(h)/\cos\theta$ , the intensity at each rock depth  $h$  can be written as

$$I_0(h) = \left( \frac{1}{\Delta\Omega \Delta t \epsilon} \right) \frac{\sum_i N_i m_i}{\sum_i A_i / \cos\theta_i}, \quad (1)$$

where  $N_i$  is the observed number of events for each of the bins at rock depth  $h$ ,  $m_i$  is the number of muons

per event,  $\theta_i$  is the zenith angle, and  $A_i$  is the projected area of the detector. In addition,  $\epsilon$  is the trigger and reconstruction efficiency and  $\Delta t$  is the live-time. In this equation the sums have been taken over all bins for which  $h_i$  is within  $\pm 50/2 \text{ hg cm}^{-2}$  of  $h$ . For this data sample the efficiency  $\epsilon$  was estimated to be 98% and is independent of direction

The observed angular distribution has been studied at each depth interval; within the errors it behaves linearly with  $\sec\theta$ . At our minimum depth of 3250 m.w.e. the upper limit on the prompt component is 10%

Fig. 3 shows the vertical intensity distribution. In this figure the data include the multimueon component in order to compare our results with those of other experiments [6–9]. In addition the data have been corrected for efficiencies and rock composition. Preliminary geological surveys yield for the Gran Sasso rock an average density of  $2.71 \pm 0.05 \text{ g cm}^{-3}$ , and rock parameters  $\langle Z \rangle = 11.4$ ,  $\langle Z/A \rangle = 0.498$  and  $\langle Z^2/A \rangle = 5.7$ . Since these parameters are somewhat different from standard rock ( $Z=11$ ,  $A=22$ ), a correction was applied following the procedure described in ref. [10].

The errors shown in fig. 3 have been estimated solely from statistical fluctuations; the errors are consistent with the spread of the intensity values for different angular bins corresponding to the same rock thickness. Consequently the systematic uncertainties due to variations in rock density, or other local effects, are smaller than the statistical uncertainty. For the variations of the average density over paths of  $\sim 1$

km,  $\Delta\rho/\rho < 7\%$ .

The intensity shown in fig. 3 is in reasonable agreement with previous measurements at overlapping depths [7–9] within systematic and statistical uncertainties. Our overall systematic error is at present between 5 and 10%; it arises mainly from the uncertainties in the rock composition.

The data points in fig. 3 have been fit to the simple phenomenological exponential form [7]

$$I_0(h) = A \exp(-h/h_0), \quad (2)$$

yielding  $A = (1.19 \pm 0.05) \times 10^{-6} \text{ cm}^{-2} \text{ s}^{-1} \text{ sr}^{-1}$ ,  $h_0 = (757 \pm 6) \text{ hg cm}^{-2}$  and  $\chi^2/\text{DoF} = 46/41$ . The errors quoted, as well as those given below, are purely statistical. The exponential form is adequate to describe the data over the depth range shown in fig. 3.

A fit of the data to the form used by the Frejus experiment [8]

$$I_0(h) = B(h_1/h)^2 \exp(-h/h_1), \quad (3)$$

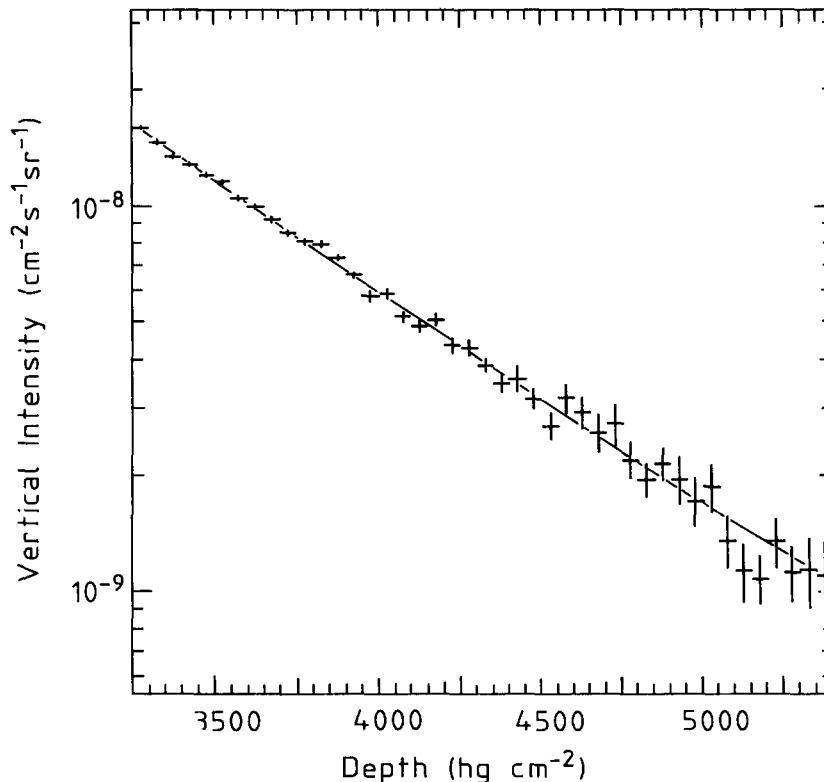


Fig. 3 Measured vertical flux for muons crossing ten planes of the MACRO detector as a function of rock thickness. The line represents a fit of the data to formula (3) (see text)

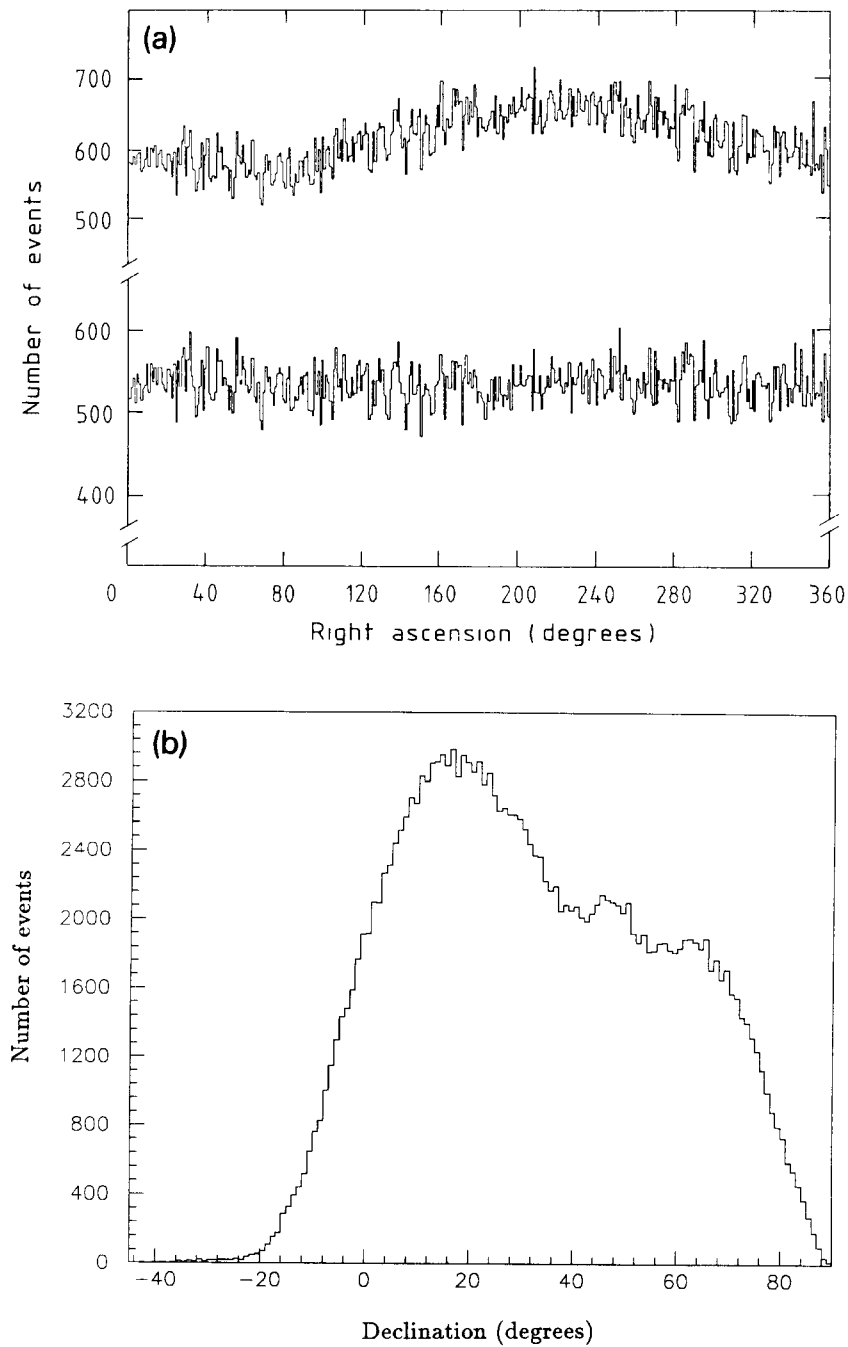


Fig 4 (a) Distributions in right ascension for single muons, before (top distribution) and after correction (bottom distribution) for the live-time of the apparatus (b) Declination distribution for single muons after live-time correction

yields  $B = (1.50 \pm 0.06) \times 10^{-6} \text{ cm}^{-2} \text{ s}^{-1} \text{ sr}^{-1}$ ,  $h_1 = (1250 \pm 10) \text{ hg cm}^{-2}$  and  $\chi^2/\text{DoF} = 52/41$ .

The parameters of the muon spectrum, assumed to follow a simple power law,  $dN/dE_\mu = KE_\mu^{-\gamma}$  for  $E_\mu > 1$  TeV, can be extracted from the underground vertical muon intensity [9]. Using the muon survival probability  $P(h, E_\mu)$  [11], folded with the assumed form of the spectrum, the intensity can be written as

$$I(h) = K \int_0^\infty P(h, E_\mu) E_\mu^{-\gamma} dE_\mu. \quad (4)$$

A fit of the data of fig. 3 using eq. (4) and the assumed power law yields  $dN/dE_\mu = (6 \pm 1) \times E_\mu^{(-3.56 \pm 0.03)} \text{ cm}^{-2} \text{ s}^{-1} \text{ sr}^{-1} \text{ GeV}^{-1}$  with  $\chi^2/\text{DoF} = 50/41$ . The error on the slope is only statistical; the systematic error is about of the same order.

By replacing the survival probability curve with a step function whose value is 1 for muon energies greater than  $E_{\text{min}} = \alpha [\exp(\beta h) - 1]$ , we have  $I_0(h) = K_1 [\exp(\beta h) - 1]^{-\gamma+1}$ , where  $K_1 = K\alpha^{1-\gamma}/(\gamma-1)$ . Using  $\beta = 0.4 \times 10^{-3} \text{ m.w.e.}^{-1}$  [12], a fit to our data gives  $K = (5 \pm 1)$  and  $\gamma - 1 = (2.55 \pm 0.03)$ , with a  $\chi^2/\text{DoF} = 52/41$ .

In the above fits systematic errors have not been included. Nevertheless, the parameters of these fits agree reasonably well with the parameters determined by other experiments.

### 3.2. Search for large scale anisotropies

To increase the statistical accuracy the data cuts have been relaxed to include all single muon tracks in which at least four planes of streamer tubes were hit. The total number of events in this sample is approximately 245 000.

The data were analyzed to search for large scale anisotropies in the muon distribution in celestial coordinates. While the distribution in declination of the events reflects the mountain shape and the acceptance of the apparatus, the distribution in right ascension is expected to be flat after live-time correction, in the absence of anisotropies. The live-time correction was made by rejecting events with a probability proportional to the distribution of live side-real time, normalizing to the interval with the smallest number of events [13]. Fig. 4a shows the distributions in right ascension of all muons before

(245 000) and after (192 250) the live-time correction. Fig. 4b shows the declination distribution for 192 250 single muons.

The amplitude of the first Fourier harmonic of the right ascension sample corrected for live-time was computed as

$$r_1 = \frac{2}{N} \left( \sum_i \cos \alpha_i \right)^2 + \left( \sum_i \sin \alpha_i \right)^2, \quad (5)$$

where  $\alpha_i$  is the right ascension of the  $i$ th event and  $N$  is the total number of muons. For this sample,  $r_1 = 4 \times 10^{-3}$ , which yields an upper limit of  $8 \times 10^{-3}$  (95% CL) in the amplitude of the first harmonic of a possible large scale anisotropy [14]. For an isotropic distribution

$$P(r > r_0) = \exp\left(\frac{-r_0^2 N}{4}\right), \quad (6)$$

for any  $r_0$ . For our data  $P = 46\%$ . With the same procedure the amplitude of the second Fourier harmonic is  $r_2 = 2 \times 10^{-3}$ ; the probability to obtain by chance a value greater than  $r_2$  is 81%. At our depth single muons come mainly from cosmic ray primaries of energies of  $\approx 10^{13}$  eV [15]. Although this analysis yields no evidence for large scale anisotropies, our upper limit is not in conflict with the positive measurement reported in ref. [16].

## 4. Conclusions

In conclusion, downward muon data have been analyzed from the first run of the first supermodule of MACRO. The variation of the vertical muon intensity has been measured for rock depths in the range  $3200 < h < 5200 \text{ hg cm}^{-2}$ . The results reported here agree with previous determinations at other depths. In addition, a preliminary search has been made for large scale anisotropies.

## Acknowledgement

We gratefully acknowledge the technical support provided by the Gran Sasso National Laboratory and by our home Institutions. This work was supported

in part by the Department of Energy and the National Science Foundation.

## References

- [1] A. Zichichi, *The Gran Sasso project*, Proc Intern Workshop ICOMAN 83 (Frascati, 1983),  
E. Bellotti, *Underground Physics and the Gran Sasso National Laboratory*, Proc 3rd ESO/CERN Symp. (Kluwer Academic Publisher, Dordrecht, 1988).
- [2] G. Battistoni et al, *Nucl Instrum. Methods A* 270 (1988) 185.
- [3] M. Calicchio et al, *Proc 20th ICRC (Moscow)*, Vol 6 (1987) p 500
- [4] M. Calicchio et al, *Nucl Tracks Radiat Meas* 15 (1988) 331
- [5] I. D'Antone et al, *IEEE Trans Nucl Sic* 36 (1989) 1602
- [6] J. W. Elbert et al, *Phys Rev D* 27 (1983) 1448
- [7] G. Battistoni et al, *Nuovo Cimento* 9C (1986) 197
- [8] Ch. Berger et al, *Phys Rev D* 40 (1989) 2163
- [9] L. Bergamasco et al., *Nuovo Cimento* 6C (1983) 569
- [10] A.G. Wright, *Proc. 12th ICRC (Denver, USA)*, Vol 3 (1973) p 1709,  
G. Auriemma, *The rock overburden of the Gran Sasso Laboratory*, *Macro Internal Note* (1990),  
H. Bilokon, *Atomic number calculation for the Gran Sasso rock*, *Macro Internal Note* (1990)
- [11] H. Bilokon et al, *Proc 20th ICRC (Moscow)*, Vol 9 (1987) p 199
- [12] T. K. Gaisser and T. Stanev, *Nucl Instrum Methods A* 235 (1985) 183,  
J. Babson et al, *ICR-report 205-89-22* (1989), *Phys Rev D*, to be published
- [13] S. Louruu, *Proc 20th ICRC (Moscow)*, Vol. 2 (1987) p 27
- [14] J. Linsley, *Phys Rev Lett* 34 (1975) 1530
- [15] H. Bilokon et al, *Proc 21st ICRC (Adelaide)*, Vol 9 (1990) p 366
- [16] Yu. M. Andrejev et al, *Proc 20th ICRC (Moscow)*, Vol 2 (1987) p 22